Innovative Food Science and Emerging Technologies 39 (2017) 171–178

Contents lists available at ScienceDirect

Innovative Food Science and Emerging Technologies

journal homepage: www.elsevier.com/locate/ifset

Performance comparison between the free running oscillator and 50 Ω radio frequency systems

Hongxue Zhou [a], Chengyang Guo [a], Shaojin Wang [a,b,*]

[a] Northwest A&F University, College of Mechanical and Electronic Engineering, Yangling, Shaanxi 712100, China
[b] Department of Biological System Engineering, Washington State University, 213 L.J. Smith Hall, Pullman, WA 99164-6120, USA

ARTICLE INFO

Article history:
Received 19 October 2016
Received in revised form 27 November 2016
Accepted 3 December 2016
Available online 15 December 2016

Keywords:
RF system
Performance
Milled rice
Heating rate
Heating uniformity
Energy efficiency

ABSTRACT

Two common kinds of radio frequency (RF) systems (free running oscillator and 50 Ω) are widely applied in industry and research. However, their unclear performances based on different operational mechanisms influence effective implementations of the two systems. The purpose of this research was to explore advantages and disadvantages of the two systems by experimental comparison. The results showed that heating rates and energy efficiency of the free running oscillator RF system were higher than those of the 50 Ω RF system under the same conditions (e.g. powers, electrode gaps, sample sizes and moisture contents), but control accuracy of the 50 Ω RF system was better than that of the free running oscillator RF system since its RF power could be adjusted under the same electrode gap. The RF heating uniformity and stability of the 50 Ω RF system were also better than those of the free running oscillator RF system. These comparison results may provide detailed performance information of the two RF systems and help to promote further practical applications of the two RF systems in food processing industry.

1. Introduction

Radio frequency (RF) heating is a technology using electromagnetic wave between 1 and 300 MHz for baking (Koral, 2004; Palazoglu, Coskun, Kocadagli, & Gokmen, 2012), cooking (Laycock, Piyasena, & Mittal, 2003), thawing (Farag, Duggan, Morgan, Cronin, & Lyng, 2009; Farag, Lyng, Morgan, & Cronin, 2008, 2011; Marra, Zhang, & Lyng, 2009), drying (Lee, Li, Zhao, & Park, 2010; Marshall & Metaxas, 1999; Wang, Zhang, Gao, et al., 2014a; Wang, Zhang, Johnson, et al., 2014b; Zhang, Zheng, Zhou, Huang, & Wang, 2016), pasteurization (Gao, Tang, Villa-Rojas, Wang, & Wang, 2011; Kim, Sagong, Choi, Ryu, & Kang, 2012) and disinfestation (Alfaifi et al., 2014; Hou, Ling, & Wang, 2014; Lagunas-Solar et al., 2007; Shrestha & Baik, 2013; Wang, Monzon, Johnson, Mitcham, & Tang, 2007a, 2007b; Wang, Tiwari, Jiao, Johnson, & Tang, 2010; Zhou, Ling, Zheng, Zhang, & Wang, 2015; Zhou & Wang, 2016a, 2016b). To avoid the interruption with communications, a frequency of 27.12 MHz has been commonly used for RF systems in food processing industries and research laboratories. In recent years, RF treatments have been increasingly studied because of the rapid heating, large power penetration depth, and high energy efficiency (Jiao, Tang, Wang, & Koral, 2014; Liu, Yang, & Mao, 2010; Piyasena, Dussault, Koutchma, Ramaswamy, & Awuah, 2003; Wang, Zhu, Chen, Li, & Wang, 2015).

There are two kinds of RF systems (the free running oscillator and 50 Ω RF systems) frequently used for researches and industrial applications. The basic heating principle of RF systems is using ever-changing electromagnetic fields to heat dielectric materials and caused mainly by ionic conductance and dipole rotation (Nelson, 1996; Zhu, Yan, Huang, Li, & Wang, 2014). The free running oscillator system consists of transformer, rectifier, oscillator, an inductance-capacitance pair commonly referred to as the "tank circuit", and the work circuit. Transformer, rectifier, oscillator and "tank circuit" are called 'RF generator'. The transformer raises the voltage and the rectifier changes the alternating current to direct current, which is then converted by the oscillator into RF energy. Parallel plate electrodes with a sample load in between act as a capacitor in the work circuit (Zhu, Yan, Huang, Li, & Wang, 2014). The 50 Ω RF system has similar structure with the free running oscillator RF system. In the 50 Ω system, however, a crystal oscillator provides a weak signal at a stable frequency (e.g., 27.12 MHz), which is subsequent amplified and transmitted through a coaxial cable to the applicator. An impedance-matching network is automatically tuned to maintain a fixed impedance of 50 Ω in the applicator's circuit to ensure that maximum coupling of energy is achieved. With a matching system, therefore, the 50 Ω RF system can allow and optimize power transfer from the generator to the product (SAIREM, 2015). The free running oscillator RF systems have been widely applied to research labs including disinfesting walnuts (Wang, Monzon, Johnson, Mitcham, & Tang, 2007b), in-shell almonds (Gao, Tang, Villa-Rojas, Wang, & Wang, 2011), and pistachios (Ling, Hou, Li, & Wang, 2016), or industries such

* Corresponding author.
E-mail address: shaojinwang@nwsuaf.edu.cn (S. Wang).

http://dx.doi.org/10.1016/j.ifset.2016.12.003
1466-8564/

as drying leather (Balakrishnan, Vedaraman, Sundar, Muralidharan, & Swaminathan, 2004), processing cookies and snack foods (Koral, 2004). The 50 Ω RF system has been used in thawing beef meats (Farag et al., 2008, 2009, 2011), and pasteurizing vacuum-packaged ham slices (Orsat, Bai, Raghavan, & Smith, 2004), and pork luncheon roll meat emulsion (Marra, Lyng, Romano, & McKenna, 2007). The proper and effective applications are dependent on exploring the unique performance of the two RF systems.

The major performance of RF heating systems includes heating rate, heating uniformity, energy efficiency and system stability. Some performances of the RF system have been studied, such as heating rate of chestnuts under different gaps (Hou, Ling, & Wang, 2014), heating uniformity in wheat flour and nut products (Tiwari, Wang, Tang, & Birla, 2011) and energy efficiency of milled rice (Zhou & Wang, 2016a) using free running oscillator RF systems. However, the major performance parameters are not completely covered in above studies. Most importantly, the advantages and disadvantages of the two RF systems have not been systematically compared, resulting in limited applications of the two RF systems and renewed interests to promote further practical applications of the two RF systems in food processing industry.

The objectives of this study were (1) to compare the temperature-time history and heating rate in selected milled rice when subjected to the two RF systems in different conditions (electrode gaps, sample weights, and moisture contents), (2) to study the heating uniformity of the milled rice in the two RF systems with varying electrode gaps, and (3) to analyze the energy efficiency and stability of the two RF systems under different electrode gaps.

2. Materials and methods

2.1. Materials and sample preparation

Milled rice (*Oryza sativa L.*) used in the study was purchased from a local market in Yangling, Shaanxi, China. The initial moisture content of milled rice was 12.3% wet basis (w.b.). The original samples were conditioned by direct addition of a predetermined amount of distilled water to obtain the target moisture contents, e.g. 15.3% w.b. for heating rate tests. The preconditioned samples were gently mixed and shaken for 15 min. Then the samples were sealed in air-tight plastic bags and stored at 4 °C for 4 d in a refrigerator (BD/BC-297KMQ, Midea Refrigeration Division, Hefei, China) to allow the moisture to equilibrate. During the storage, the bags were shaken 4 times per day. After that, the sample bags could be taken out from the refrigerator (Guo, Tiwari, Tang, & Wang, 2008; Guo, Wang, Tiwari, Johnson, & Tang, 2010; Rani, Chelladurai, Jayas, White, & Kavitha-Abirami, 2013; Wang, Zhu, Chen, Li, & Wang, 2015). All the milled rice samples including moisture contents of 12.3% and 15.3% w.b. in plastic bags were kept in an incubator (BSC-150, Boxun Industry & Commerce Co., Ltd., Shanghai, China) to equilibrate at 25 ± 0.5 °C for one day before the experiment.

2.2. RF heating systems

The free running oscillator (SO6B, Strayfield International, Wokingham, U.K., Fig. 1) and 50 Ω (RF labotron, Sairem, Neyron, France, Fig. 2) RF systems were used for heating experiment. The free running oscillator RF system was described in detail by Wang et al. (2010), Zheng, Zhang, Zhou, & Wang (2016), and Zhou, Ling, Zheng, Zhang, and Wang (2015). The electrode gap was set up to obtain required heating rate or RF power. The 50 Ω RF system also had two parallel plate electrodes and a hot air system for surface heating, but the function to setup the input power. The specific parameters of the two RF systems are shown in Table 1. It was obvious that the cavity volume and electrode gap range of 50 Ω RF system were smaller than those of the free running oscillator system due to different power level. The performance parameters of the two RF systems were compared under their commonly used conditions.

2.3. RF heating procedure

2.3.1. Separated layer of sample

The preconditioned samples were taken from the incubator rapidly to have the same initial temperature (25 °C) before RF treatment. The 3.9 kg rice samples with 6 cm in depth divided equally into three layers and separated by two thin gauzes (with mesh opening of 1 mm) were placed in the center of bottom electrode to easily map the sample surface temperatures at heights of 2, 4 and 6 cm (Fig. 3) after RF treatment. Five electrode gaps of 90, 95, 100, 105 and 110 mm were selected for comparison tests, without conveyor belt movement and hot air heating.

2.3.2. Electric current and power setup

The anode currents (I, A) of the free running oscillator system were read directly from the control screen and recorded when the RF heating was conducted. This electric current was used to calculate the RF power (P, kW) with a relationship ($P = 5 \times I - 1.5$) provided by the manufacturer (Hou et al., 2014; Jiao, Johnson, Tang, & Wang, 2012; Zhou et al., 2015). Average power of three experiments applied in the free running oscillator system for reducing the error caused by varying RF power was used to set up the RF power of the 50 Ω RF system under the same electrode gap. The corresponding powers for the two RF systems were 1758, 1450, 1058, 866, and 650 W under the electrode gaps of 90, 95, 100, 105 and 110 mm, respectively. Besides, when RF systems heated 3.9, 2.9, and 1.9 kg milled rice in the same container and electrode gap of 100 mm, the used RF powers were 1450 W, 850 W, and 450 W, respectively. The maximum RF voltage of the top electrode which is an important physical parameter to form electromagnetic field between two plates and measured by senor in the system was read and recorded immediately for the 50 Ω RF system. Meanwhile, it could indirectly reflect heating process when RF system worked.

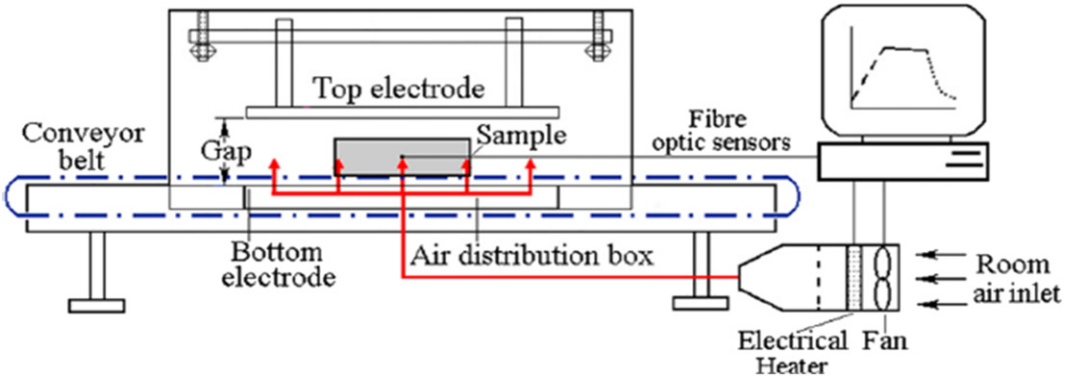

Fig. 1. Schematic view of the free running oscillator RF system showing the plate electrodes, conveyor belt, and the hot air system (adapted from Wang, Tiwari, Jiao, Johnson, & Tang, 2010).

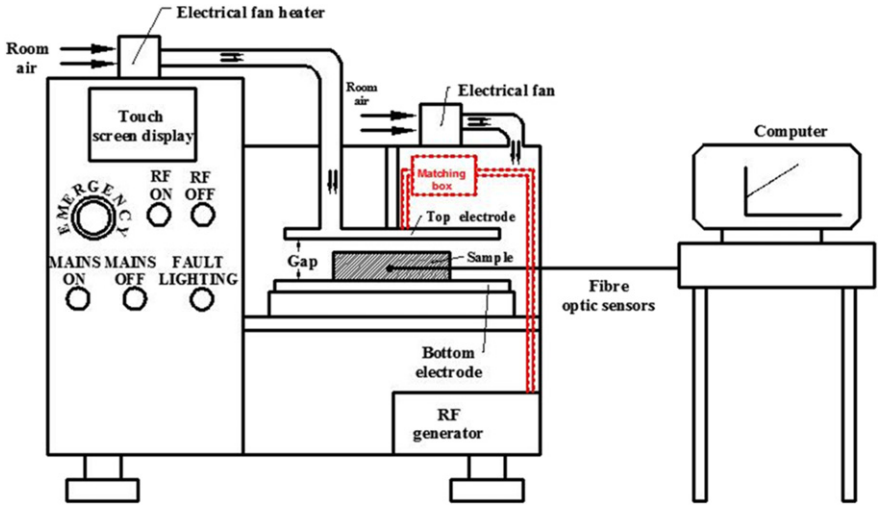

Fig. 2. Schematic view of the 50 Ω RF system showing the plate electrodes, control panel and the hot air system.

2.3.3. Heating procedure

Before the RF heating, the initial sample surface temperatures in three layers were measured sequentially by a thermal imaging camera (DM63, Zhejiang Dali Technology Co., Ltd., Hangzhou, China) with an accuracy of ±2 °C. During the RF heating, sample temperature in the center (Fig. 3) of the container was measured by fiber optic sensors (FTS-P104, HeQiopto-Electronic Technology, Xi'an, Shanxi, China) with an accuracy of ±1 °C. When the sample temperature at the geometric center of the sample reached 50 °C (Zhou et al., 2015), the RF system was turned off and samples in container were immediately moved out for the surface temperature measurement. Each thermal image took <1 s. Details on the infrared imaging system to measure product surface temperatures after RF treatment can be found in Wang et al. (2006). From each of the thermal images, the surface temperature data in the RF heated sample were obtained and used for calculating the average temperature and standard deviation (SD), which were further used for statistical analyses (Wang et al., 2007b; Wang, Tang, Johnson, & Cavalieri, 2013; Wang, Yue, Tang, & Chen, 2005; Wang et al., 2015). Each test was repeated three times.

2.4. RF heating uniformity tests under different electrode gaps

Non-uniform heating is a major problem in developing effective RF treatment. Heating uniformity index (λ) has been proposed by Wang, Yue, Chen, & Tang (2008) and Wang, Yue, Tang, and Chen (2005) to estimate temperature distributions of heating samples in the RF treatment. This index λ has been successfully used for evaluating RF heating uniformity in walnuts (Wang, Monzon, Johnson, Mitcham, & Tang, 2007a), legumes (Wang et al., 2010), lentils (Jiao, Johnson, Tang, & Wang, 2012), coffee beans (Pan, Jiao, Gautz, Tu, & Wang, 2012), almonds (Gao, Tang, Wang, Powers, & Wang, 2010), chestnuts (Hou et al., 2014), rice (Zhou et al., 2015; Zhou & Wang, 2016b), and corns (Zheng, Zhang, Zhou, & Wang, 2016). Heating uniformity index is defined as the ratio of the rise in standard deviation of sample temperatures to the rise in average sample temperatures during RF treatment and can be calculated by the following equation (Wang, Yue, Chen, & Tang, 2008):

$$\lambda = \frac{\sqrt{\sigma^2 - \sigma_0^2}}{\mu - \mu_0} \quad (1)$$

where μ_0 and μ are initial and final mean temperatures (°C) of milled rice, σ_0 and σ are initial and final standard deviations (°C) of milled rice temperatures over RF heating time, respectively. The smaller values represent the better RF heating uniformity.

2.5. Energy efficiency of the two RF systems

The energy efficiency is an important parameter to measure RF system performances and can be calculated as the ratio of the total energy absorbed by product (P_{output}, W) to the power input (P_{input}, W) (Jiao et al., 2012; Wang et al., 2007a). The energy efficiency (η, %) of the RF systems was calculated by the following equation:

$$\eta = P_{ouput}/P_{input} \times 100\% = mC_\rho(\Delta T/\Delta t)/P_{input} \times 100\% \quad (2)$$

where m is the mass of milled rice (kg), C_P is the specific heat of rice samples (1.69 kJ/kg °C) at room temperature (Iguaz et al., 2003; Zhou

Table 1
Major parameters of the free running oscillator and 50 Ω RF systems.

Parameter	Systems	
	Free running oscillator	50 Ω
RF power (kW)	6	2.4
Frequency (MHz)	27.12	27.12
Electrode size (mm)	830 × 400	600 × 400
Electrode gap (mm)	90–190	50–220
Hot air temperature (°C)	20–70	20–60
Overall dimensions (m)	3.5 × 2.1 × 2.1	1.3 × 0.9 × 2.0
Conveyor speed (m/h)	1.0–60	–
Monitored parameters	Current (A)	Voltage (V) RF power Matching

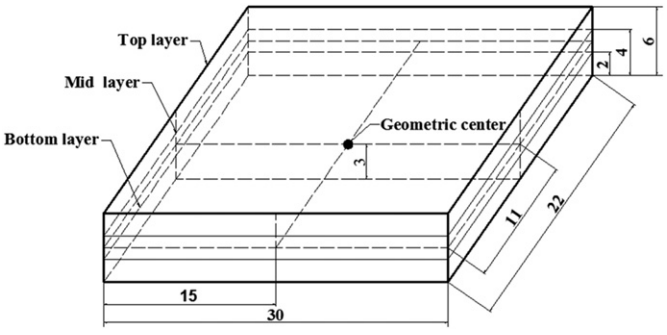

Fig. 3. Rectangular plastic container with 3 layers for sample temperature measurements (all dimensions are in cm) (Zhou et al., 2015).

& Wang, 2016a), ΔT is the rise in mean temperature (°C) over treatment time Δt (s), and P_{input} is an input power (W) calculated by the read electric current (I, A) for the free running oscillator system and a set-point of RF power for the 50 Ω RF system.

2.6. Stability of the RF systems

The stability of the RF systems refers mainly to characteristics of power changes due to variations in sample temperature and dielectric properties during the RF treatments. To clearly evaluate the system stability, ΔP was used to evaluate the systems stability and calculated by the following equation:

$$\Delta P = P_{max} - P_{min} \quad (3)$$

where P_{max} and P_{min} are the maximum and minimum powers (W) over the RF heating time, respectively. The smaller ΔP values represent the better stability of the RF system.

3. Results and discussion

3.1. Electric current of the free running oscillator RF system under different electrode gap

Fig. 4 shows the relationship between the electric current and the electrode gap when the plastic container filled with 3.9 kg milled rice at 12.3% w.b. was placed on the center of RF bottom electrode without movement and forced hot air. With rice, the electric current decreased rapidly from 0.67 A to 0.43 A when electrode gap increased from 90 mm to 110 mm, and then decreased slowly when the electrode gap changed from 110 mm to 190 mm. The similar trends were also found by Gao, Tang, Wang, Powers, and Wang (2010), Hou et al. (2014), Jiao et al. (2012), Zhou et al. (2015) and Zheng et al. (2016).

3.2. Electric voltage of the 50 Ω RF system under different electrode gaps

Fig. 5 shows the relationship between the electric voltage and the electrode gap under the same conditions with the free running oscillator system. With milled rice, the electric voltage decreased rapidly from 1984 V to 1560 V when electrode gap increased from 90 mm to 110 mm. However, when the electrode gap increased from 110 mm to 190 mm, the voltage decreased slowly. The trend of electric voltage change was similar to that of electric current in the free running oscillator RF system.

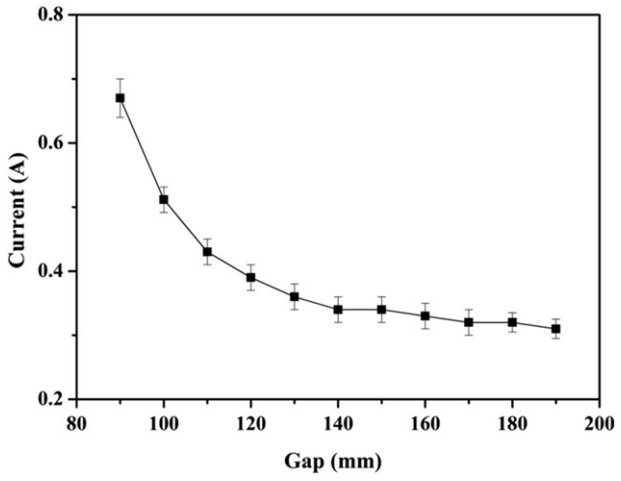

Fig. 4. Electric current of the free running oscillator RF system as a function of electrode gap.

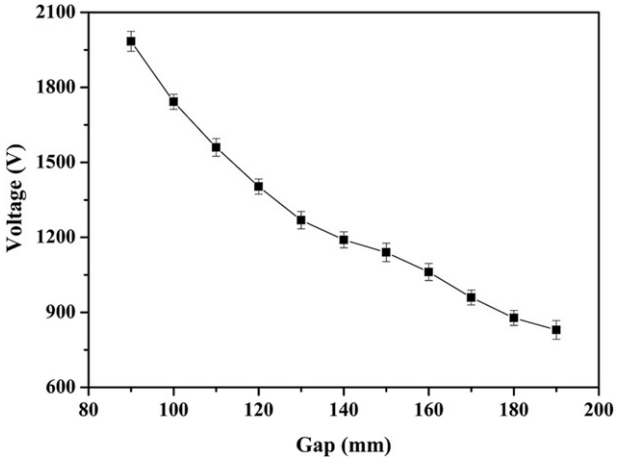

Fig. 5. Voltage of the 50 Ω RF system as a function of electrode gap.

3.3. Comparison of heating rate in the center of milled rice sample

3.3.1. Heating rates under different electrode gaps

The temperature histories of the 3.9 kg milled rice with 12.3% w.b. in free running oscillator RF system using five electrode gaps are shown in Fig. 6a. The milled rice temperatures increased almost linearly with heating time under five gaps. The heating rates increased with decreasing electrode gaps or increasing RF power because the gap was lower, or RF power was greater resulting in the electromagnetic field being stronger. About 2.0, 2.7, 3.3, 4.3, and 5.2 min were needed to heat the 3.9 kg milled rice from 25 °C to 50 °C for the electrode gaps of 90, 95, 100, 105, and 110 mm, respectively. For the 50 Ω RF system (Fig. 6b), about 3.0, 4.0, 5.3, 7.0, and 8.7 min were needed for heating the milled rice samples to achieve 50 °C under the gaps of 90, 95, 100, 105, and 110 mm, respectively. The 50 Ω RF system resulted in longer time to achieve the same target temperature and provided slower heating rates at each electrode gap as compared to the free running oscillator RF system.

3.3.2. Heating rates under different sample weights

Fig. 7 shows the comparison of the temperature-time histories at the geometric center of milled rice sample with 12.3% w.b. during the RF heating using three different sample weights at the electrode gap of 95 mm. The heating rates of milled rice samples with 3.9, 2.9, and 1.9 kg for the free running oscillator RF system were 9.4, 6.3, and 4.0 °C min^{-1}, respectively, as compared to 6.8, 5.0, and 2.4 °C min^{-1} for the 50 Ω RF system. The heating rates decreased with decreasing weights for both RF systems. It was observed again that the heating rates in the free running oscillator RF system were faster than those of the 50 Ω RF system under the same weights.

3.3.3. Heating rates under different moisture contents

Fig. 8 shows the comparison of the temperature-time histories at the geometric center of 3.9 kg milled rice sample during the RF heating under two moisture contents at the electrode gap of 100 mm. The estimated RF powers were 1400 W and 1058 W for the moisture contents of 15.3% and 12.3% w.b., respectively, suggesting that the more RF power was absorbed by the higher moist products (Zhang, Zhu, & Wang, 2015). About 2.8 and 3.3 min were needed to heat the 3.9 kg milled rice with 15.3% and 12.3% w.b. from 25 °C to 50 °C, respectively, in the free running oscillator RF system, resulting in heating rates of 8.8 and 7.5 °C min^{-1}. Moreover, the 50 Ω RF system took 4.5 and 5.3 min to heat the same sample from 25 °C to 50 °C with two moisture contents of 15.3 and 12.3% w.b. under the same conditions, respectively, with corresponding heating rates of 5.6 and 4.7 °C min^{-1}. The results showed that the heating rate value in the free running oscillator RF system were

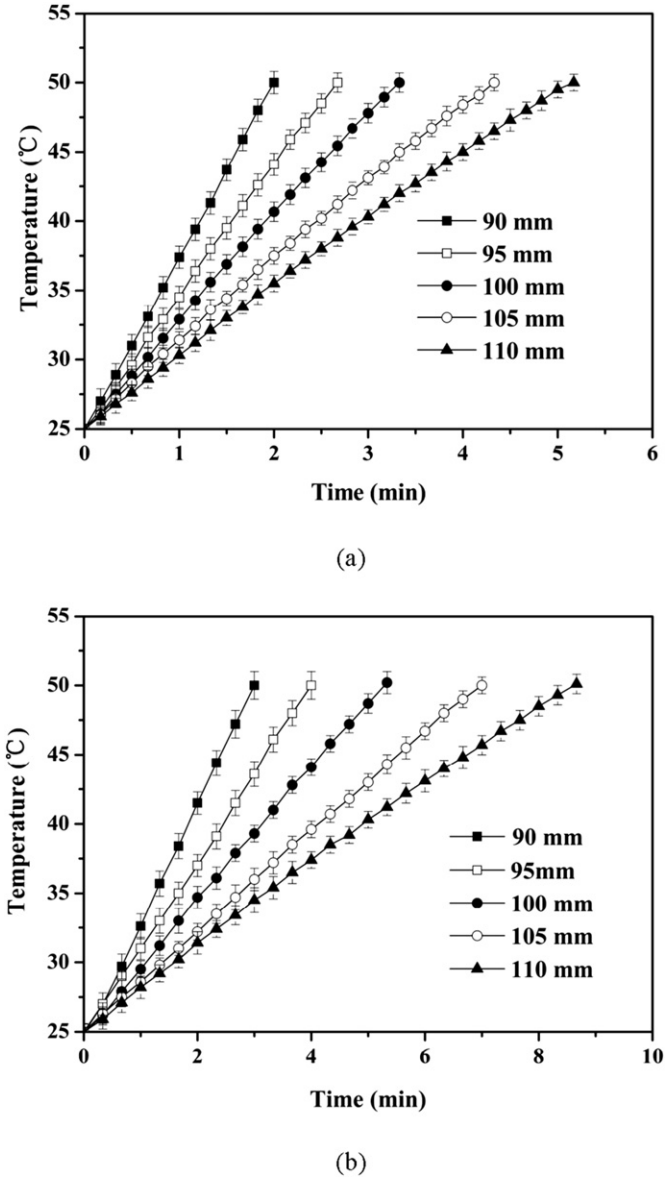

Fig. 6. Temperature-time histories of the free running oscillator (a) and 50 Ω RF (b) systems heated 3.9 kg milled rice samples with 12.3% w.b. in the center of containers as a function of the electrode gap.

higher than that in the 50 Ω RF system in the same moisture contents under the same conditions.

3.3.4. Heating rates as influenced by power and electrode gap in the 50 Ω RF system

Fig. 9 shows the relationship between heating rates and RF power (800, 1600, and 2400 W) and electrode gaps (90, 95, 100, 105, and 110 mm) after 50 Ω RF treatment. For the given milled rice samples, overall heating rates were larger than those of the geometric center under the same electrode and RF power. This is probably caused by the edge and corner overheating (Wang et al., 2010, 2013). Besides, the heating rate difference between the overall and the geometric center decreased with increasing electrode gaps and RF power. The influence of electrode gap on heating rate increased with increasing RF power. The maximum heating rate reached 12.5 °C min^{-1} with RF power of 2400 W and electrode gap of 90 mm.

The RF power of the 50 Ω RF system could be adjusted to any value from 0 to 2400 W with a control accuracy (minimum range of power adjustment) of 1 W under any electrode gaps (50–220 mm). The intrinsic

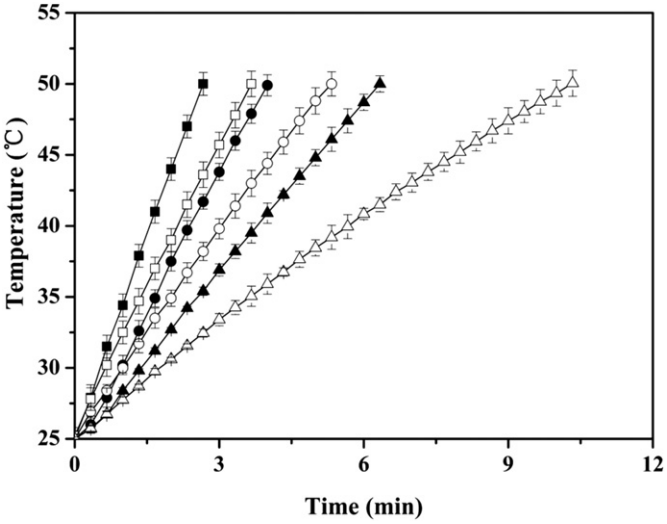

Fig. 7. Temperature-time histories of milled rice in the free running oscillator (solid) and 50 Ω (hollow) RF systems as function of sample mass (3.9 kg (square), 2.9 kg (cycle), and 1.9 kg rice (triangle)) with 12.3% w.b.

maximum RF power of the free running oscillator RF system was 6 kW and controlled by electrode gaps with a control accuracy of 50 W, but the maximum RF power used was only 2 kW when heated 3.9 kg milled rice (12.3% w.b.) under the given electrode gaps (90–190 mm). The actual RF power varied with the operational conditions (e.g. gaps) and sample status (e.g. moisture) in the free running oscillator system. Control accuracy of the 50 Ω RF system was better than that of the free running oscillator RF system.

3.4. Heating uniformity comparison between the two systems

Fig. 10a provides the relations between uniformity index (λ) and electrode gaps (90, 100, and 110 mm) of the free running oscillator RF system after RF treatment. The uniformity index and standard deviation of milled rice decreased with increasing gaps. The best uniformity was observed in the bottom layer, which was located at the lowest layer of container and followed by the middle and top layers because the surface temperature of top layers was lost too much to air. The uniformity index

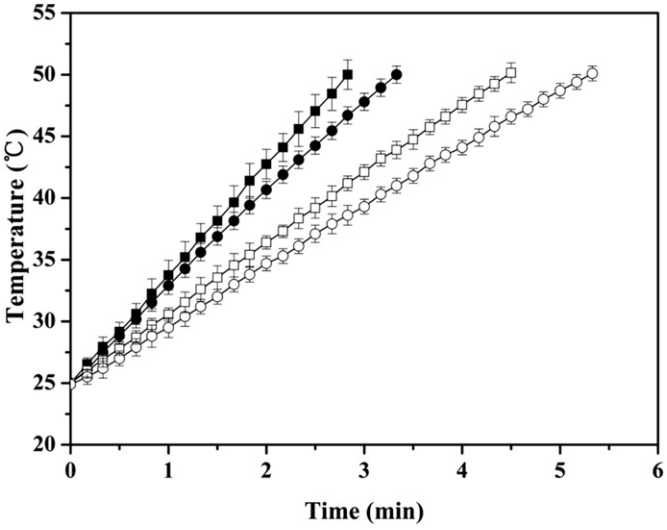

Fig. 8. Temperature-time histories of 3.9 kg milled rice in the free running oscillator (solid) and 50 Ω (hollow) RF systems as a function of sample moisture content (15.3% w.b. (square) and 12.3% w.b. (cycle)).

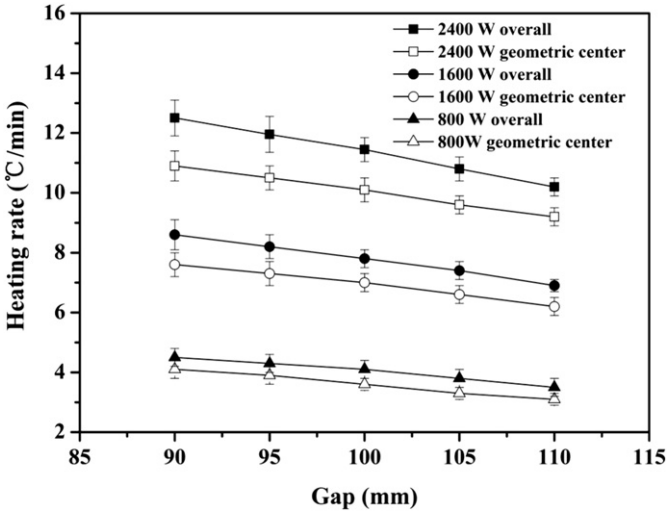

Fig. 9. Heating rate of with 3.9 kg milled rice (12.3% w.b.) in the 50 Ω RF system as a function of power and electrode gap.

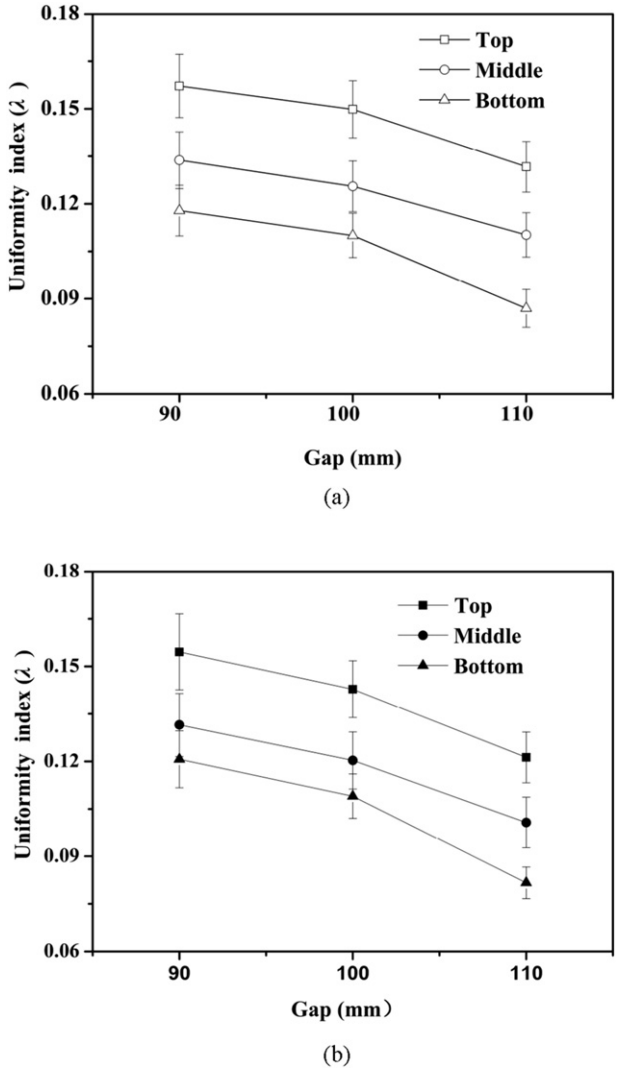

Fig. 10. Heating uniformity index in 3.9 kg milled rice (12.3% w.b.) after the free running oscillator (a) and 50 Ω (b) RF system heating as a function of the electrode gap.

values in this study were similar to those reported by Zhou et al. (2015), Zhou & Wang, (2016a), and Zhou & Wang, (2016b).

Fig. 10b shows the relations between uniformity index (λ) and electrode gaps (90, 100, and 110 mm) of the 50 Ω RF system from 25 °C to 50 °C after RF treatment. The trend of uniformity with varying gaps was similar to uniformity indexes in wheat flour and nut products (Tiwari, Wang, Tang, & Birla, 2011;Wang et al., 2007a, b; Hou et al., 2014). The 50 Ω RF system had smaller uniformity index and standard deviation in sample temperatures, suggesting better heating uniformity as compared to the free running oscillator RF system.

3.5. Energy efficiency comparison of the two systems

Fig. 11 shows the estimated heating efficiency of the two RF systems with five electrode gaps (90, 95, 100, 105, and 110 mm) at the sample moisture content of 12.3% w.b. The heating efficiency decreased with increasing electrode gaps. According to Eq. (2), RF energy efficiency of the free running oscillator RF system were 79.4%, 78.4%, 76.5%, 74.2% and 73.4% under the electrode gaps of 90, 95, 100, 105, and 110 mm, respectively. The observed heating efficiency values in this study were comparable with 79.5% for RF treated walnuts (Wang et al., 2007a), 76.5% for lentils (Jiao et al., 2012), and 75.2–76.3% for three types of rice (Zhou & Wang, 2016a). By increasing sample moisture content, the energy efficiency would be slightly raised since the increased specific heat and heating rate could be balanced by the increased input power.

Similarly, the energy efficiency of the 50 Ω RF system also decreased with increasing electrode gaps. The observed heating efficiency values in this study were also comparable with <60% for RF treated roll meat emulsion (Romano & Marra, 2008). Besides, the energy efficiency of the free running oscillator RF system was higher than that of the 50 Ω RF system under the same moisture content because of the heating rate value in the free running oscillator RF system being higher than that in the 50 Ω RF system under the same conditions. Thus, the energy efficiency of the 50 Ω RF system was lower than that of the free running oscillator RF system, which was probably caused by energy loss due to complicated matching regulations.

3.6. Stability of the two systems

Table 2 shows RF power (P_{max} and P_{min}) and ΔP of the two systems. Generally, the mean values of ΔP decreased with increasing electrode gaps for the free running oscillator RF system. There was no significant difference in ΔP ($p > 0.05$) among the electrode gaps due to large power variations except between 90 mm or 100 mm and 110 mm

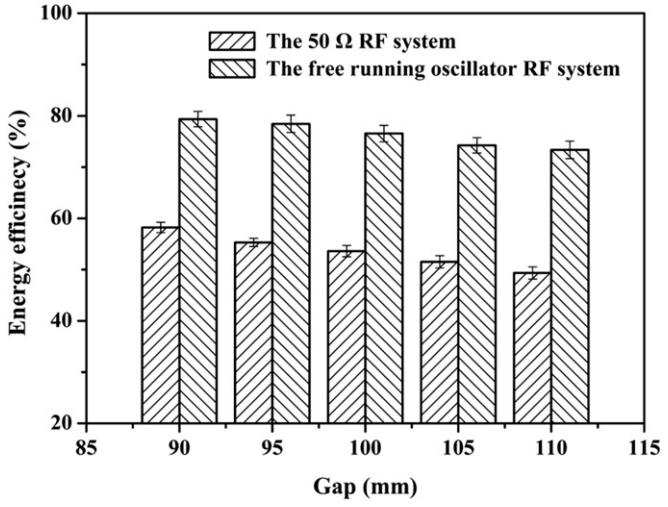

Fig. 11. Heating efficiency of 3.9 kg milled rice (12.3% w.b.) in the free running oscillator and 50 Ω RF systems as a function of the electrode gap.

Table 2
RF system power (W) changes in the heating process with sample moisture content of 12.3% w.b.

RF systems		Gap (mm)														
		90			95			100			105			110		
Free running oscillator	Times	P_{max}	P_{min}	ΔP	P_{max}	P_{min}	ΔP	P_{max}	P_{min}	ΔP	P_{max}	P_{min}	ΔP	P_{max}	P_{min}	ΔP
	Rep 1	1750	1550	200	1400	1350	50	1150	1000	150	950	800	150	650	600	50
	Rep 2	1950	1800	150	1550	1300	250	1100	1000	100	900	850	50	700	650	50
	Rep 3	1850	1650	200	1650	1450	200	1150	950	100	950	750	200	650	650	0
	Avg	1850	1666	183	1533	1367	167	1133	983	117	933	800	133	667	633	33
	± SD	± 100	± 125	± 28a[*s]	± 126	± 76	± 104ab	± 29	± 29	± 29a	± 29	± 50	± 76ab	± 29	± 29	± 29bc
50 Ω	Rep 1	1758	1758	0	1450	1450	0	1058	1058	0	866	866	0	650	650	0
	Rep 2	1758	1758	0	1450	1450	0	1058	1058	0	866	866	0	650	650	0
	Rep 3	1758	1758	0	1450	1450	0	1058	1058	0	866	866	0	650	650	0

* Mean values in ΔP are not significantly different ($p > 0.05$) for the same letter within a row among the electrode gap.

($p < 0.05$). Similarly, the free running oscillator RF system also showed its instability under different moisture contents (Table 3). Maximal power variation reached 250 W in the free running oscillator RF system as compared to null changes in the 50 Ω RF system. The heating rate decrease was often found in the free running oscillator RF system due to reduced power (Hou et al., 2014). But the automatic RF power drop is useful to avoid product quality degradation due to maintaining relatively low sample temperatures for RF drying. The 50 Ω RF system was very stable during the RF treatment periods with the advanced control strategy, which is useful to keep the required sample temperature constant for pasteurization and disinfestations.

4. Conclusions

Performance between the free running oscillator and 50 Ω RF systems was compared by experiment based on their heating principles. The volume of the free running oscillator system which could be estimated by L (m) × W (m) × H (m) was 6.9 times as much as that of the 50 Ω RF system. Heating rates and energy efficiency of the free running oscillator RF system were higher than those of the 50 Ω RF system under the same conditions (e.g. electrode gaps, sample size and moisture contents), but control accuracy of the 50 Ω RF system was better than that of the free running oscillator RF system since its RF power could be adjusted under the same electrode gap. The RF heating uniformity and stability of the 50 Ω RF system were better than those of the free running oscillator RF system. This study may provide clear information and guidelines for appropriate selections of applying the RF heating systems.

Acknowledgements

This research was conducted in the College of Mechanical and Electronic Engineering, Northwest A&F University, and supported by research grants from General Program of National Natural Science Foundation of China (no. 31371853), 948 Program of Ministry of Agriculture of China (2014-Z21) and Open Fund from Zhejiang Academy of Agricultural Science (2010DS700124-ZM1605). The authors gratefully thank to Ajuan Zheng, Liang Zhao, Teng Cheng, Liyang Zhou, Bo Zhang, Bo Ling, Zhi Huang and Rui Li for their helps and suggestions in conducting experiments.

Table 3
RF system power (W) changes under the electrode gap of 100 mm with two moisture contents.

RF Systems	Moisture contents	12.3% w.b.			15.3% w.b.		
Free running oscillator	Times	P_{max}	P_{min}	ΔP	P_{max}	P_{min}	ΔP
	Rep 1	1150	1000	150	1450	1300	150
	Rep 2	1100	1000	100	1500	1350	150
	Rep 3	1150	950	100	1450	1350	100
50 Ω	Rep 1	1058	1058	0	1400	1400	0
	Rep 2	1058	1058	0	1400	1400	0
	Rep 3	1058	1058	0	1400	1400	0

References

Alfaifi, B., Tang, J., Jiao, Y., Wang, S., Rasco, B., Jiao, S., & Sablani, S. (2014). Radio frequency disinfestation treatments for dried fruit: Model development and validation. *Journal of Food Engineering, 120*, 268–276.

Balakrishnan, P. A., Vedaraman, N., Sundar, V. J., Muralidharan, C., & Swaminathan, G. (2004). Radio frequency heating - A prospective leather drying system for future. *Drying Technology, 22*(8), 1969–1982.

Farag, K. W., Lyng, J. G., Morgan, D. J., & Cronin, D. A. (2008). Dielectric and thermophysical properties of different beef meat blends over a temperature range of −18 to +10 degrees C. *Meat Science, 79*(4), 740–747.

Farag, K. W., Duggan, E., Morgan, D. J., Cronin, D. A., & Lyng, J. G. (2009). A comparison of conventional and radio frequency defrosting of lean beef meats: Effects on water binding characteristics. *Meat Science, 83*(2), 278–284.

Farag, K. W., Lyng, J. G., Morgan, D. J., & Cronin, D. A. (2011). A comparison of conventional and radio frequency thawing of beef meats: Effects on product temperature distribution. *Food and Bioprocess Technology, 4*(7), 1128–1136.

Gao, M., Tang, J., Wang, Y., Powers, J., & Wang, S. (2010). Almond quality as influenced by radio frequency heat treatments for disinfestation. *Postharvest Biology and Technology, 58*(3), 225–231.

Gao, M., Tang, J., Villa-Rojas, R., Wang, Y., & Wang, S. (2011). Pasteurization process development for controlling Salmonella in in-shell almonds using radio frequency energy. *Journal of Food Engineering, 104*(2), 299–306.

Guo, W., Tiwari, G., Tang, J., & Wang, S. (2008). Frequency, moisture and temperature-dependent dielectric properties of chickpea flour. *Biosystems Engineering, 101*(2), 217–224.

Guo, W. C., Wang, S. J., Tiwari, G., Johnson, J. A., & Tang, J. (2010). Temperature and moisture dependent dielectric properties of legume flour associated with dielectric heating. *LWT- Food Science and Technology, 43*(2), 193–201.

Hou, L., Ling, B., & Wang, S. (2014). Development of thermal treatment protocol for disinfesting chestnuts using radio frequency energy. *Postharvest Biology and Technology, 98*, 65–71.

Iguaz, A., San Martin, M. B., Arroqui, C., Fernandez, T., Mate, J. I., & Virseda, P. (2003). Thermophysical properties of medium grain rough rice (LIDO cultivar) at medium and low temperatures. *European Food Research and Technology, 217*(3), 224–229.

Jiao, S., Johnson, J. A., Tang, J., & Wang, S. (2012). Industrial-scale radio frequency treatments for insect control in lentils. *Journal of Stored Products Research, 48*, 143–148.

Jiao, Y., Tang, J., Wang, S. J., & Koral, T. (2014). Influence of dielectric properties on the heating rate in free-running oscillator radio frequency systems. *Journal of Food Engineering, 120*, 197–203.

Kim, S. Y., Sagong, H. G., Choi, S. H., Ryu, S., & Kang, D. H. (2012). Radio-frequency heating to inactivate Salmonella Typhimurium and *Escherichia coli* O157:H7 on black and red pepper spice. *International Journal of Food Microbiology, 153*(1–2), 171–175.

Koral, T. (2004). *Radio frequency heating and post-paking Biscuit World7 (4). (pp. 1–6), 1–6.*

Lagunas-Solar, M. C., Pan, Z., Zeng, N. X., Truong, T. D., Khir, R., & Amaratunga, K. S. P. (2007). Application of radio frequency power for non-chemical disinfestation of rough rice with full retention of quality attributes. *Applied Engineering in Agriculture, 23*(5), 647–654.

Laycock, L., Piyasena, P., & Mittal, G. S. (2003). Radio frequency cooking of ground, comminuted and muscle meat products. *Meat Science, 65*(3), 959–965.

Lee, N. H., Li, C. Y., Zhao, X. F., & Park, M. J. (2010). Effect of pretreatment with high temperature and low humidity on drying time and prevention of checking during radio-frequency/vacuum drying of Japanese cedar pillar. *Journal of Wood Science, 56*(1), 19–24.

Ling, B., Hou, L., Li, R., & Wang, S. (2016). Storage stability of pistachios as influenced by radio frequency treatments for postharvest disinfestations. *Innovative Food Science & Emerging Technologies, 33*, 357–364.

Liu, Y., Yang, B., & Mao, Z. (2010). Radio frequency technology and its application in agro-product and food processing. *Transactions of the CSAE, 41*(8), 115–120.

Marra, F., Lyng, J., Romano, V., & McKenna, B. (2007). Radio-frequency heating of foodstuff: Solution and validation of a mathematical model. *Journal of Food Engineering, 79*(3), 998–1006.

Marra, F., Zhang, L., & Lyng, J. G. (2009). Radio frequency treatment of foods: Review of recent advances. *Journal of Food Engineering*, *91*(4), 497–508.
Marshall, M. G., & Metaxas, A. C. (1999). Radio frequency assisted heat pump drying of crushed brick. *Applied Thermal Engineering*, *19*(4), 375–388.
Nelson, S. O. (1996). Review and assessment of radio-frequency and microwave energy for stored-grain insect control. *Transactions of the ASABE*, *39*(4), 1475–1484.
Orsat, V., Bai, L., Raghavan, G. S. V., & Smith, J. P. (2004). Radio-frequency heating of ham to enhance shelf-life in vacuum packaging. *Journal of Food Process Engineering*, *27*(4), 267–283.
Palazoglu, T. K., Coskun, Y., Kocadagli, T., & Gokmen, V. (2012). Effect of radio frequency postdrying of partially baked cookies on acrylamide content, texture, and color of the final product. *Journal of Food Science*, *77*(5), E113–E117.
Pan, L., Jiao, S., Gautz, L., Tu, K., & Wang, S. (2012). Coffee bean heating uniformity and quality as influenced by radio frequency treatments for postharvest disinfestations. *Transactions of the ASABE*, *55*(6), 2293–2300.
Piyasena, P., Dussault, C., Koutchma, T., Ramaswamy, H. S., & Awuah, G. B. (2003). Radio frequency heating of foods: Principles, applications and related properties - A review. *Critical Reviews in Food Science and Nutrition*, *43*(6), 587–606.
Rani, P. R., Chelladurai, V., Jayas, D. S., White, N. D. G., & Kavitha-Abirami, C. (2013). Storage studies on pinto beans under different moisture contents and temperature regimes. *Journal of Stored Products Research*, *52*, 78–85.
Romano, V., & Marra, F. (2008). A numerical analysis of radio frequency heating of regular shaped foodstuff. *Journal of Food Engineering*, *84*(3), 449–457.
SAIREM (2015). *Instruction Manual RF Labotron 2.4 kW 27.12 MHz RI 1650.* Neyron France: 12 Porte du Grand Lyonwww.sairem.com
Shrestha, B., & Baik, O. D. (2013). Radio frequency selective heating of stored-grain insects at 27.12 MHz: A feasibility study. *Biosystems Engineering*, *114*(3), 195–204.
Tiwari, G., Wang, S., Tang, J., & Birla, S. L. (2011). Analysis of radio frequency (RF) power distribution in dry food materials. *Journal of Food Engineering*, *104*(4), 548–556.
Wang, S., Yue, J., Tang, J., & Chen, B. (2005). Mathematical modelling of heating uniformity for in-shell walnuts subjected to radio frequency treatments with intermittent stirrings. *Postharvest Biology and Technology*, *35*(1), 97–107.
Wang, S., Tang, J., Sun, T., Mitcham, E. J., Koral, T., & Birla, S. L. (2006). Considerations in design of commercial radio frequency treatments for postharvest pest control in in-shell walnuts. *Journal of Food Engineering*, *77*(2), 304–312.
Wang, S., Monzon, A., Johnson, J. A., Mitcham, E. J., & Tang, J. (2007a). Industrial-scale radio frequency treatments for insect control in walnuts I: Heating uniformity and energy efficiency. *Postharvest Biology and Technology*, *45*(2), 240–246.
Wang, S., Monzon, M., Johnson, J. A., Mitcham, E. J., & Tang, J. (2007b). Industrial-scale radio frequency treatments for insect control in walnuts II: Insect mortality and product quality. *Postharvest Biology and Technology*, *45*(2), 247–253.
Wang, S., Yue, J., Chen, B., & Tang, J. (2008). Treatment design of radio frequency heating based on insect control and product quality. *Postharvest Biology and Technology*, *49*(3), 417–423.
Wang, S., Tiwari, G., Jiao, S., Johnson, J. A., & Tang, J. (2010). Developing postharvest disinfestation treatments for legumes using radio frequency energy. *Biosystems Engineering*, *105*(3), 341–349.
Wang, S., Tang, J., Johnson, J. A., & Cavalieri, R. P. (2013). Heating uniformity and differential heating of insects in almonds associated with radio frequency energy. *Journal of Stored Products Research*, *55*, 15–20.
Wang, Y., Zhang, L., Gao, M., Tang, J., & Wang, S. (2014a). Pilot-scale radio frequency drying of macadamia nuts: Heating and drying uniformity. *Drying Technology*, *32*(9), 1052–1059.
Wang, Y., Zhang, L., Johnson, J., Gao, M. X., Tang, J., Powers, J. R., & Wang, S. J. (2014b). Developing hot air-assisted radio frequency drying for In-shell macadamia nuts. *Food and Bioprocess Technology*, *7*(1), 278–288.
Wang, K., Zhu, H., Chen, L., Li, W., & Wang, S. (2015). Validation of top electrode voltage in free-running oscillator radio frequency systems with different moisture content soybeans. *Biosystems Engineering*, *131*, 41–48.
Zhang, P. Z., Zhu, H. K., & Wang, S. J. (2015). Experimental evaluations of radio frequency heating in low-moisture agricultural products. *Emirates Journal of Food and Agriculture*, *27*(9), 662–668.
Zhang, B., Zheng, A., Zhou, L., Huang, Z., & Wang, S. (2016). Developing hot air-assisted radio frequency drying for in-shell walnuts. *Emirates Journal of Food and Agriculture*, *28*(7), 459–467.
Zheng, A., Zhang, B., Zhou, L., & Wang, S. (2016). Application of radio frequency pasteurization to corn (*Zea mays* L.): Heating uniformity improvement and quality stability evaluation. *Journal of Stored Products Research*, *68*, 63–72.
Zhou, L., & Wang, S. (2016a). Industrial-scale radio frequency treatments to control *Sitophilus oryzae* in rough, brown, and milled rice. *Journal of Stored Products Research*, *68*, 9–18.
Zhou, L., & Wang, S. (2016b). Verification of radio frequency heating uniformity and *Sitophilus oryzae* control in rough, brown, and milled rice. *Journal of Stored Products Research*, *65*, 40–47.
Zhou, L., Ling, B., Zheng, A., Zhang, B., & Wang, S. (2015). Developing radio frequency technology for postharvest insect control in milled rice. *Journal of Stored Products Research*, *62*, 22–31.
Zhu, H., Yan, R., Huang, Z., Li, R., & Wang, S. (2014). Experimental studies on leaked electromagnetic fields around radio frequency heating systems. *Applied Engineering in Agriculture*, *30*(4), 601–608.